Chapter 2
Field Tests

2.1 Introduction

Being safe, comfortable, and fast, subway becomes essential in urban transportation. The vibration problem induced by subway operation also should be paid attention. There are a variety of models to analyze the ground vibration caused by the subway loading (Alabi 1992; Lipen and Chigarev 1998; Sheng et al. 1999; Jones et al. 2000). Some papers (Pan et al. 1995; Hirokazu et al. 2001; Xie et al. 2002) studied the dynamic response of track system under subway traffic loading, which is concentrated in the superstructure, and foundation soils are rarely involved. Currently, dynamic responses of the saturated soft clay around the subway tunnel have not been studied yet at home and abroad, while greater deformation of saturated soft clay soil is generated under long-term subway traffic load (Chen et al. 2002; Wang et al. 2003). According to some relevant field monitoring data, large axial deformation and surface settlement occurred in some tunnel segments of Line 1, Shanghai Metro (Lin et al. 2000), which bring a certain impact on the normal operation of the subway trains and threaten the safety of subway moving. The generation of settlements starts when the pore pressure and soil effective stress change (Tang et al. 2003a, b, 2005). Therefore, studying the dynamic responses of soils surrounding the subway tunnel plays a significant role in subway design, construction, and operation.

With respect to the soil dynamic characteristics under the subway load, two aspects should be considered. One is the dynamic responses of saturated soft clay under subway traffic load. It includes dynamic frequency response, soil dynamic response amplitude, and also the development in lateral and vertical directions. On the other side, it is the deformation response which is directly related to the settlement problem surrounding the subway tunnel. And this aspect is reflected by the continuous monitoring of pore pressure. The pore pressure response in saturated soft clay is much sensitive to the subway traffic load. The properties are various as

Y. Tang et al., *Dynamic Response and Deformation Characteristic of Saturated Soft Clay under Subway Vehicle Loading*, Springer Environmental Science and Engineering, DOI 10.1007/978-3-642-41987-4_2, © Science Press Ltd, Beijing and Springer-Verlag Berlin Heidelberg 2014

to different soil types. Even for the same soil, the pore pressure varies distinctly as well due to different load properties. Previously, the pore pressure development characteristics of saturated sand are studied really in deep in all kinds of loads. Wang et al. (2004) analyzed the pore pressure properties in sandy mixture soil under cyclic load and established the relationship between pore pressure and energy loss. Zhang and Meng (2003) focused on the excess pore pressure in saturated sand due to impact loads. The critical impact strength to reach full liquefaction of sands is discussed. Zhang et al. (2003) simulated the earthquake response in clayey layer underlying silts and sands. The excess pore pressure increase was figured out by his simulation. Bai (2003) and Yang et al. (2002) computed and analyzed the pore pressure development in saturated layers under dynamic compaction load and blasting load, respectively. Okada and Nemat-Nasser (1994) demonstrated the reasonability of the pore pressure prediction by energy loss from the soil structure view.

The research on saturated soft clay is on the very starting stage as to sands due to the complex particle composition, physical properties, and pore pressure kinetic laws in soft clay. The accumulation and dissipation of excess pore pressure under traffic loading are both relatively slower. Xu et al. (1997) investigated the pore pressure increase of saturated soft clay under undrained cyclic loading through laboratory tests. Because of the cyclic traffic load, the pore pressure in clayey soils changed regularly with some special laws. And to figure out all these characteristics, continuous monitoring of pore pressure along the depth and also in different locations is needed for the relevant data analysis.

Previous scholars were concentrated in the theoretical analysis based on the laboratory tests. The field tests are really rare. Our research group declares that the most convincible analysis and laboratory tests should be on the basis of the field monitoring data, which can be the best descriptions and suitable to leading the mechanism study. Hence, in this chapter, pore pressure and earth pressure transducers were buried along the depth in boreholes and distributed laterally in different locations as well. As the subway advanced, the earth pressure and pore pressure were real-time monitored and recorded. The development of earth pressure and pore pressure under subway traffic loading was figured out based on the field data. The comparisons at various depths and along the lateral distances are both discussed.

2.2 Engineering Geology of Soft Soil in Shanghai

The soft soil is distributed widely, even omnipresent in Shanghai, which is typical soft sediment area located on the deltaic deposit of the Yangtze River estuary and formed in coastal marshes. The subsoil in Shanghai is composed of approximately 300 m loose Quaternary sediments with small regular variety at depths (Xu et al.

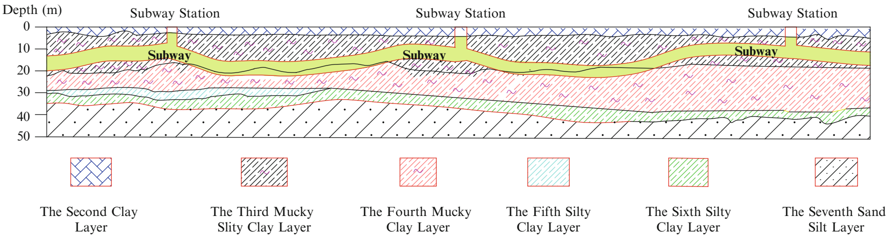

Fig. 2.1 The typical geological strata of Shanghai

2009), which consists of clay, loam, silt, and sand that vary from an estuarine to fluviatile sedimentation process. All the features and characteristics of these deposits show the physiographic evolution of the estuarine system. With the rapid development of economy and technology, particularly in the underground construction in Shanghai, the infrastructures were or are being constructed in the top shallow soft clayey deposit within subsurface 120 m, mainly consisting of Dark Green Stiff Clay (known as DGSC layer in subsurface around 70 m) with the following Upper Pleistocene (Q_3) and the Upper Holocene (Q_4) (Dassargues et al. 1991; Xu et al. 2009). Generally the soft soil in Shanghai is regarded as the layers upper the DGSC (Fig. 2.1) where the issues associated with human engineering activities are mainly concentrated. Moreover, engineering construction is much directly impacted by the third mucky silty clay layer and the fourth mucky clay layer. Meantime, the fourth mucky clay is the most occurrence layer embedded by the subway construction. In most areas, these layers are buried at a depth of 5 m. The thickness of mucky clay soil is relatively huge varying from 12 to 20 m with the absence of the third layer in some parts, which has characteristics of high water content, large pore ratio, low strength, and high compressibility attributable to the special information environment.

The model soil samples in this experimental research were obtained from Tang Town of Pudong New City in Shanghai, which is the typical soft clay soil construction site in Shanghai. In the studied zone, from a lithological point of view, the DGSC is characterized by a high bearing capacity, at a depth of about 70 m. It is overlain by a sandy layer usually called second aquifer. The latest unit formed in the estuarine environment is composed of sand deposits gradually replaced by fluvial silt and clay. The first aquifer is formed here and results in really shallow groundwater level mostly situated at a depth of 1–3 m. All the strata in the study area are shown in Fig. 2.1. The adverse engineering properties such as low permeability, thixotropy, and rheology of mucky clay soil are involved by many researchers over the years (Tang et al. 2003a, b, 2008, 2010; Xie and Sun 1996; Zhou et al. 2005), while the hydrothermal properties are rarely concerned.

2.3 Program Design

2.3.1 Selection of Testing Site

The field testing site was selected to the southern side of the east end in Jing'an Temple Station of Line 2 in Shanghai Metro. The subway train advances up to People Square and down to Zhongshan Park. The schematic is shown in Fig. 2.2.

2.3.2 Selection of Testing Instruments

The dynamic monitoring system was applied in the field test. The sampling frequency can reach as high as 200 Hz, and the precision is up to 0.1 kPa, which is very sensitive in the soil response to the subway traffic loads. The dynamic monitoring system consists of resistive sensors, dynamic strain amplifier, data acquisition, and computer. All the sampling data was recorded by the computer in real time. The whole process is depicted in Fig. 2.3.

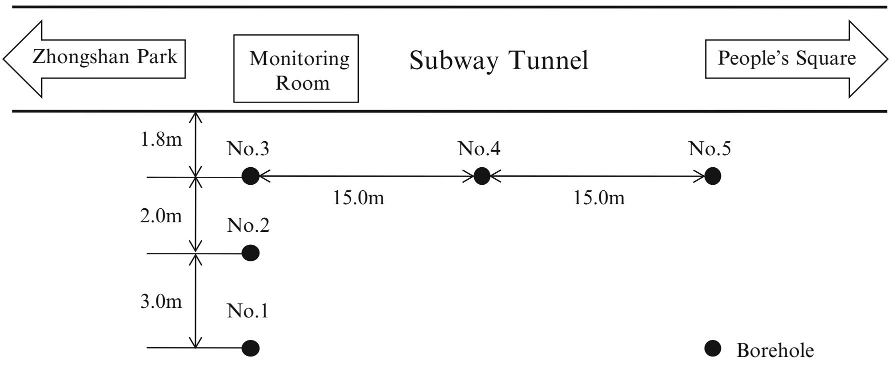

Fig. 2.2 Plan view of the testing site

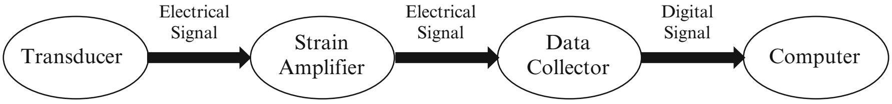

Fig. 2.3 Schematic diagram of dynamic monitoring system

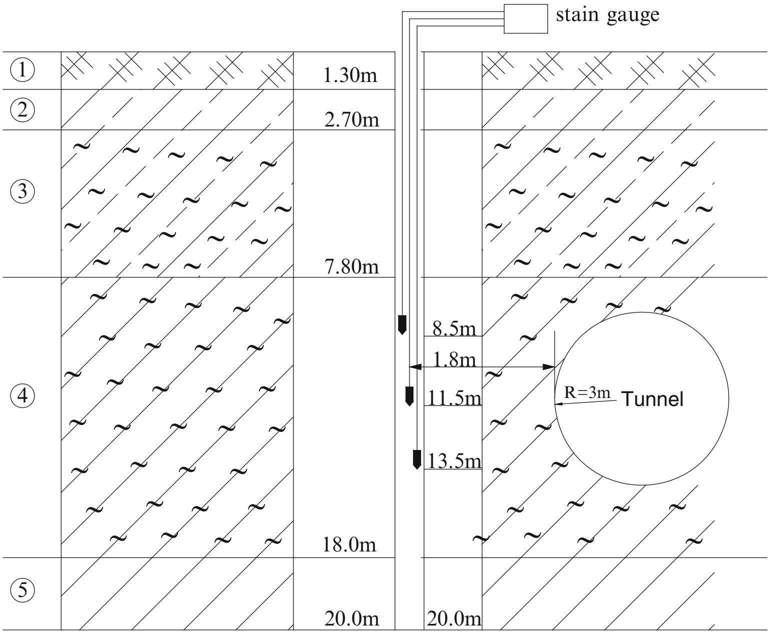

Fig. 2.4 Stratigraphic profile and instrument installation

2.3.3 Stratigraphic Section and Instrument Installation

As shown in Fig. 2.2, all the testing boreholes are distributed in line with 110 mm diameters. From a plan view, there are respectively three both parallel and perpendicular to the subway tunnel. No. 3, 4, and 5 boreholes are drilled 15.0 m apart in the tunnel axial direction with only 1.8 m offset to the tunnel segment. Perpendicularly, No. 1, 2, and 3 boreholes are distributed to study the development of soil dynamic responses to the subway traffic loads along the vertical direction. It is important to note herein that the distances between them are not always the same (shown in Fig. 2.2), which increased from 2 to 3 m. Viewed from stratigraphic section, the subway tunnel was located in the fourth layer of gray mucky clay. And all the monitoring points along the borehole are respectively 8.5 m, 11.5 m, and 13.5 m at the depths. Pressure transducers were buried in places exactly. The details of stratigraphic section and instrument installation were depicted in Fig. 2.4.

2.4 Results and Analysis

This section is to process and analyze the raw monitoring data. Some methodology is explained here. The response frequency of soft clay around the tunnel to subway traffic loads can be obtained by observing the time-domain waveform.

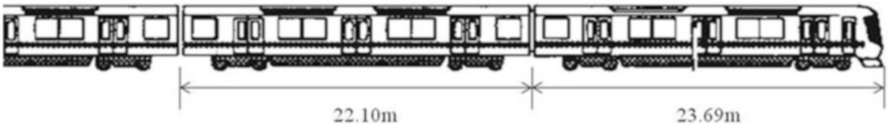

Fig. 2.5 The subway train (Model AC02) diagram of Shanghai Metro Line 2

Comprehensively observing each time-domain curve and the pore pressure development, the response characteristics of pore pressure at each depth can be figured out respectively. By comparison with the monitoring data at different measuring points along the depth, the wave propagation along the depth can be derived during the subway's operation. And the range of influence can also be simply predicted.

2.4.1 Soil Response Frequency

There are six cars in the subway train of Shanghai Metro Line 2 and the total vehicle length is 139.46 m (Fig. 2.5). The normal operation speed is 60 km/h with 30–45 s stop in each station. Since the testing site is much close to the station, the speed measured will be a little bit slower. According to the statistics, the speeds passing the measuring points are almost 30–40 km/h generally with 12–16 s duration. And in different periods, the intervals of the subway trains passing by the measuring points are different, generally 3–6 min and 3–4 min in rush hour times.

It can be easily seen in Fig. 2.5 that there are four concentrated (axle) loads in each subway car (two wheels in each end), which are transferred downward to the track structure and the foundation soil below through wheel rails. When the subway train approaches or passes the nearby measuring points, the traffic load spreads out by means of wave, and relevant response in soil can be observed.

In Fig. 2.6, the response wave when the subway train passed by one measuring point can be clearly seen. The response frequencies may be various due to different axle loads and track gauges. In a whole, two kinds of frequencies alternately showed up, which we called high frequency f_H and low frequency f_L. The most probable is that the high frequency caused by the loads of front wheels in one subway car and rear wheels in adjacent subway car periodically subjected to soils. The response time was relatively short. While as to the front wheels or rear wheels on each subway car, the cyclic loading time is longer and the response frequency is relatively low. Just as shown in the response wave figure, the soil vibration response can be easily found when each subway car approached and passed over.

To minimize surrounding impact on the data collection, 10 Hz filter was utilized in the field test. Numerous data were collected through continuous real-time monitoring. By comparing all the wave curves, a typical response wave of saturated soft clay was identified. Comprehensively summarized, conducted, and analyzed all the data, response frequencies at each depth of mucky clay soils were obtained

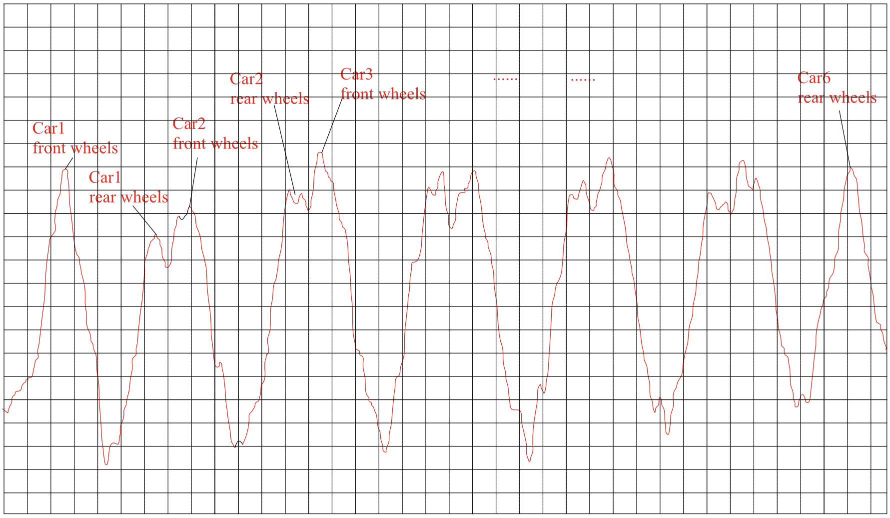

Fig. 2.6 The soil vibration response wave

Table 2.1 Frequency statistics

Measurement No.	High frequency (Hz)	Low frequency (Hz)	Measurement No.	High frequency (Hz)	Low frequency (Hz)
1-A-S	2.533	0.428	1-A-W	2.533	0.525
1-B-S	*	*	1-B-W	*	*
1-C-S	3.046	0.475	1-C-W	2.425	0.486
2-A-S	*	*	2-A-W	2.757	0.425
2-B-S	2.533	0.446	2-B-W	2.488	0.512
2-C-S	2.425	0.525	2-C-W	2.465	0.562
3-A-S	2.455	0.425	3-A-W	2.845	0.485
3-B-S	2.762	0.338	3-B-W	2.425	0.512
3-C-S	2.895	0.411	3-C-W	*	*
4-A-S	*	*	4-A-W	2.712	0.452
4-B-S	2.533	0.414	4-B-W	2.855	0.445
4-C-S	*	*	4-C-W	*	*
5-A-S	2.425	0.453	5-A-W	2.824	0.533
5-B-S	2.764	0.425	5-B-W	2.623	0.532
5-C-S	2.465	0.422	5-B-W	2.335	0.494

Note: In the Measurement No., the first number refers to borehole No.; *A*, *B*, and *C* refer to a depth of 8.5 m, 11.5 m, and 13.5 m, respectively; *S* refers to earth pressure transducer; *W* refers to pore water pressure transducer; * notes that no data were monitored in this borehole

(Table 2.1). Figure 2.7 also showed the histogram graph of response frequencies in each monitoring boreholes. Statistically, the high frequency f_H was in a range of 2.5–2.8 Hz and the low frequency f_L 0.4–0.6 Hz in value. Considering the most disadvantaged situation, 2.5 Hz was chosen in the laboratory tests.

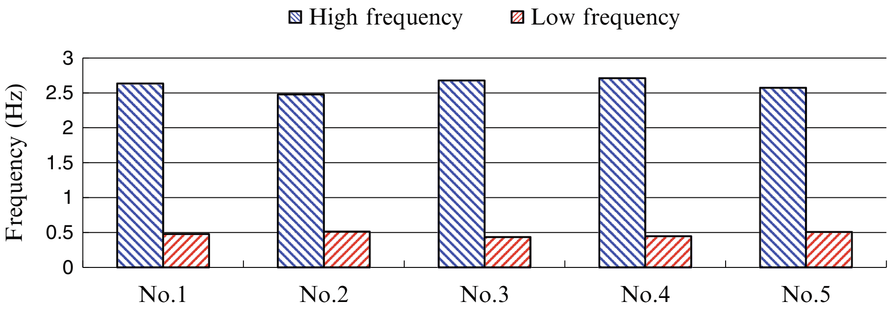

Fig. 2.7 Frequency histogram in monitoring boreholes

According to these two kinds of response frequencies from the field monitoring, combined with the natural frequency of saturated soft clay in Shanghai, some appropriate measurements should be considered to avoid similar or same frequencies between these two to resonance. If it happened, it would cause some engineering disasters such as the tunnel instability problems and segment cracking.

2.4.2 The Attenuation of Dynamic Response in Perpendicular Direction to Subway Tunnel Axis

Study on the subway traffic load involves many subjects, including locomotive dynamics, vehicle track dynamics, soil dynamics, and structure dynamics; subway tunnel is a partially enclosed space, in which subway train travels on the tracks. The wheel-rail contact force on the track structure is the main source of tunnel traffic load. It is always composed by two parts, the static load of rolling stock weight and vibration part by subway operation. The subway traffic load is generated by two aspects of both subway cars and track irregularity, in which the latter is the main reason.

In terms of vibration source mechanism, it has already a unified understanding, i.e., the high-speed operation of the subway train. It consists of two aspects of vehicles and tracks. As for the vehicle, the problem is mainly concentrated on wheels, such as wheel tread wear, wheel flat sliding, wheel out of round, and eccentric wheel, and about the track, when subway trains advance, a large number of wheel-rail contact forces conduct on the track simultaneously, which results in the vibration of wheels and track structure. Since jointless track and monolithic concrete bed are utilized in subway line, the track irregularity, especially the random irregularity, plays a great role on the vibration.

The study of attenuation development of soil dynamic response to subway load with the increase of distance from vibration source herein is firstly considered on the lateral direction. Previously, Chen et al. (1998) indicated experimentally that

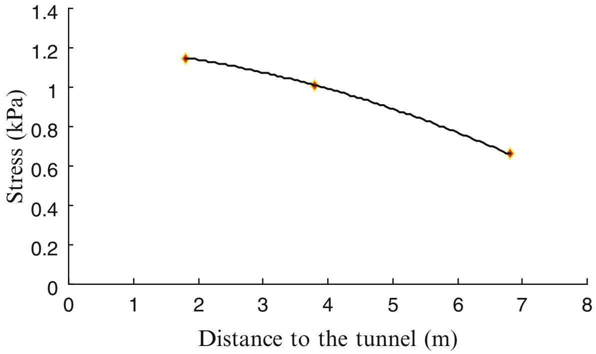

Fig. 2.8 Attenuation of lateral stress perpendicular to tunnel axis

Table 2.2 Fitting parameters

K_0	K_1	K_2
1.2122	0.0177	0.0093

the vibration was attenuated into zero at the distance of 25 m from the rail flange. Out of this range, soil dynamic response almost disappeared. Others also proved this point except the attenuation distance may vary with different traffic loads and circumstances. Meantime, buried deep in semi-infinite soils, the attenuation herein must be greater than surface. Seen in Fig. 2.1, No. 1, 2, and 3 boreholes were set in different distances from the tunnel sideline of 6.8 m, 3.8 m, and 1.8 m, respectively. To avoid the surface influences, all the transducers in different distances were located at the same depth of 13.5 m. Having comprehensively analyzed all the data in field, the results are shown in Fig. 2.8.

According to the field monitoring data and the analysis of the attenuation characteristics, the attenuation relationship with lateral distance perpendicular to tunnel axis is

$$\Delta p = K_0 - K_1 x - K_2 x^2 \tag{2.1}$$

where

Δp is the dynamic response value at distance of x (kPa)
K_0 is the dynamic response value at tunnel edge line (kPa)
K_1 is the first attenuation coefficient of dynamic response (kPa/m)
K_2 is the second attenuation coefficient of dynamic response (kPa/m^2)
x is the distance from the tunnel edge line (m)

Fitting all the monitoring data and combining regression analysis for Eq. (2.1), the parameters were obtained and presented in Table. 2.2.

Hence, the attenuation development with distances can be depicted in Eq. (2.2):

$$\Delta p = 1.2122 - 0.0177x - 0.0093x^2 \tag{2.2}$$

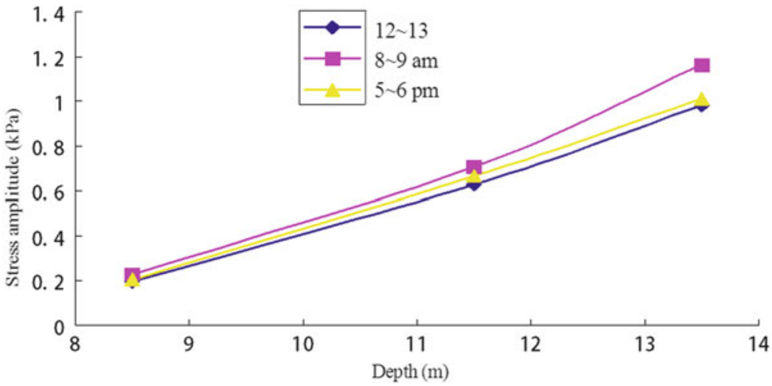

Fig. 2.9 Soil dynamic response amplitude with the depth

where, x is ranging from 0 to 11.33 m. With this formula the range of influence and the dynamic response values can be figured out. And the influence on surrounding environment can also be predicted and estimated on the basis of it.

From Fig. 2.8, as the distance increased, the soil dynamic response attenuation reflected on the dynamic stress amplitude. According to Eq. (2.2), the influence range can be calculated as 10.50 m. This result is distinct compared with the characteristics of the surface influence range of track traffic load. Besides the natural properties of soils, it's mainly because the shear modulus and damping ratio both increase along the depth.

2.4.3 The Dynamic Response Development Along the Depth

The transducers were distributed in soils around the top, axis, and bottom of subway tunnel. The early monitoring data indicated that the earth stress increased nearly linearly along the depth. During the subway operation, to figure out the relation of stress amplitude with the depth, rush hour was selected as the statistical duration for calculation. The statistical results were described in Fig. 2.9.

From Fig. 2.9, under the subway traffic loading, the biggest response was 0.23 kPa at a depth of 8.5 m, 0.7 kPa at 11.5 m, and 1.15 kPa at 13.5 m, respectively. The relation between the stress response amplitude and depth was almost linear. In addition, it can be also found that the dynamic stress responses were different in various subway operation periods, i.e., largest in the morning rush hour, second in the evening rush hour, and smallest at noon. It inferred that the passage flow during morning is largest and should be paid more attention in design and construction. The monitoring data during this period should be regarded as design reference.

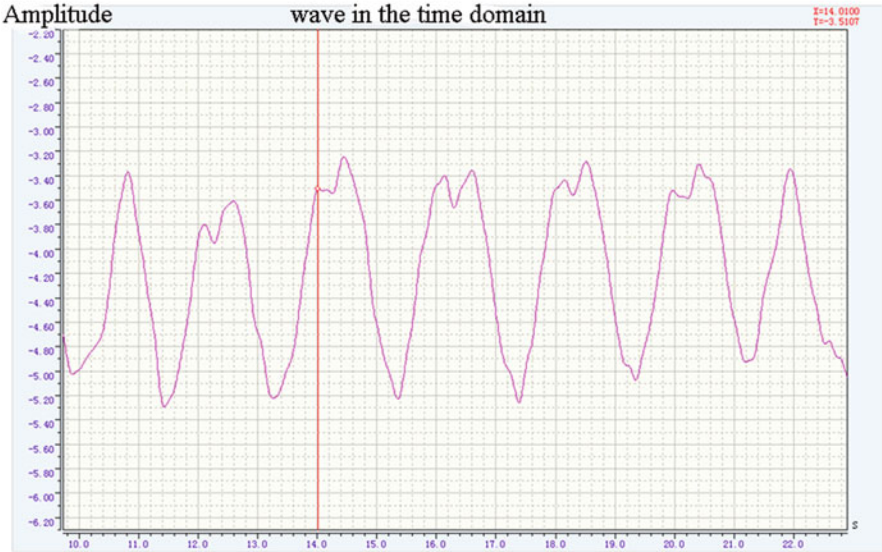

Fig. 2.10 Response curve of pore water pressure at subsurface 11.5 m

2.4.4 Development of Pore Pressure

Here taking the pore pressure development curve at a depth of 11.5 m as example to illustrate (Fig. 2.10), it described the pore pressure response curve during the subway operation, in which *y*-axis was the pore pressure response value (in $\mu\varepsilon$) and *x*-axis was time (in unit of s). According to the calibration coefficients, it can be transferred into curve of excess pore pressure verse vibration number (Fig. 2.10). With the same method, the pore pressure curves at the depths of 8.5 and 13.5 m in the location No.3 borehole were both conducted and the excess pore pressure curves were obtained (Figs. 2.12 and 2.13). From Figs. 2.11, 2.12, and 2.13, the excess pore pressure in surrounding saturated soft clay did not change a lot when the subway was advancing close, not exceeding 0.5 kPa.

The field monitoring data showed that the pore pressure dynamic response was caused by subway. It can be obviously seen that the pore pressure vibration number was just several and the amplitude was also very small. The subway operation interval was generally 3–5 min. During this time, the excess pore pressure can be almost dissipated completely. That is to say, the excess pore pressures induced by two adjacent subway cars would never superimpose. The details will be introduced in laboratory tests of the next chapter.

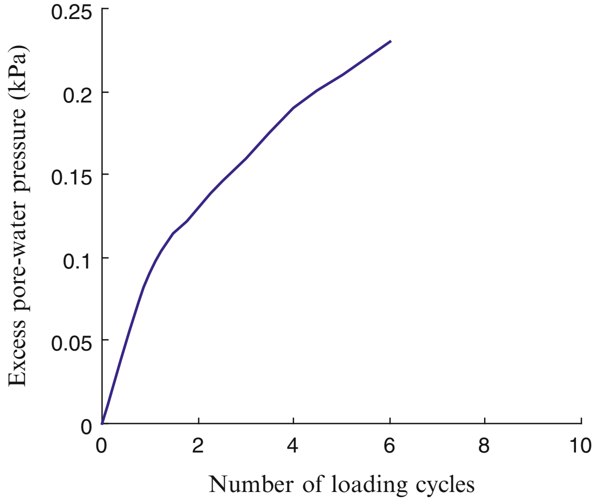

Fig. 2.11 Curves of over-static pore water pressure and vibration number at a depth of 11.5 m

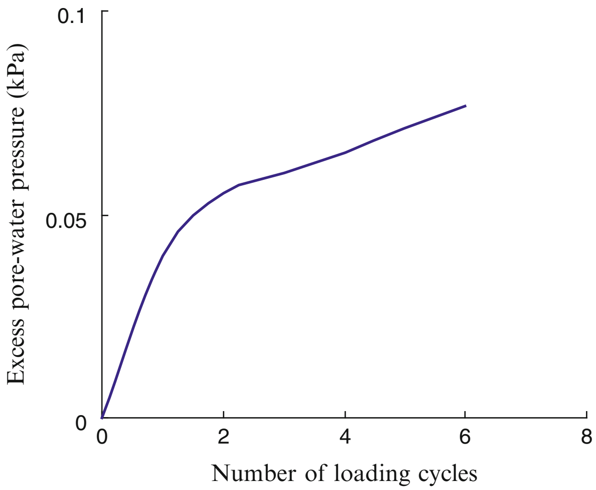

Fig. 2.12 Curves of over-static pore water pressure and vibration number at a depth of 8.5 m

2.4.5 Mechanism Analysis of Pore Pressure Development Under Subway Traffic Loading

The dynamic properties of pore pressure of saturated soft clay under subway traffic loading are characterized as follows: elastic compression occurred when the saturated soft clay subjected to traffic loads. It resulted in the rapid increase on pore pressure. After the subway passed by, the soil structure rebounded and negative

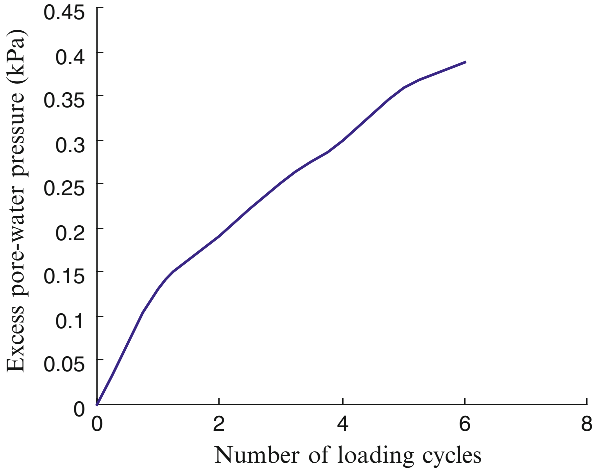

Fig. 2.13 Curves of over-static pore water pressure and vibration number at a depth of 13.5 m

pore pressure was generated and the total pore pressure decreased accordingly. As shown in Fig. 2.10, each subway train has six subway cars and each of them has four wheel sets with respective gauges of 2.8, 13.0, and 2.8 m. When each car wheel passed over the same measuring point, the increase and dissipation of pore pressure of saturated soft soil were both superposed. The dynamic response of pore pressure to the subway traffic load in each measuring point was related to the axle load transferred by wheels according to track structures. Therefore, the characteristics of pore pressure increasing and dissipating in each measuring point must correspond to the time and duration of the subway train wheel set passing each point. While times and intervals in different operation stages are various, and also there is some interference from another subway train, the pore pressure curve measured at each point is not the uniform wave curve. In the meantime, during rush hours, the amplitude of traffic load is bigger, corresponding energy transferred is greater, and the dynamic response of pore pressure is also relatively larger. All of this was reflected in Fig. 2.10. The subway traffic load was transmitted to the tunnel segment and lining structures and then transferred to surrounding soils by energy. After the interaction of soil and water, energy decayed gradually. Besides parts of energy absorbed by soils, some others were consumed by overcoming the initial hydraulic gradient of saturated soft clay to get the pore pressure increased. Once the traffic load disappeared, the pore pressure dissipated and water level recovered gradually. When the pore pressure did not dissipate completely before next train approached, the pore pressure fluctuated a lot constantly. When the subway stopped, the pore pressure dissipated and reached the final equilibrium steady state.

2.5 Chapter Summary

Subjected to the saturated soft clay surrounding tunnel areas of the Jing'an Temple Station-Jiangsu Road Station in Shanghai Line 2, continuous dynamic field monitoring was conducted by numbers of earth pressure and pore pressure transducers at different locations and depths. Some significant conclusions were obtained as follows:

1. During the subway train passing over, two dynamic response frequencies were generated in surrounding saturated soft clay. According to the measured dynamic response frequencies in soil and corresponding natural soil frequency, some appropriate measurements should be considered to avoid similar or same frequencies between these two to induce resonance, which will result in great damage to the subway tunnel.
2. In the direction perpendicular to the subway tunnel axis, the traffic load attenuated with increasing distance. The dynamic response attenuation with distance can be predicted in a formula by statistical analysis. The range of influence and the dynamic response amplitude were also obtained.
3. The dynamic response amplitude varied linearly with the depth. And the values in different rush hour stages were various, largest in the morning rush hours, secondary in the evening, and least at noon. It indicated that the passage flow was largest in the morning. During this stage, the soil was in a worst situation and the dynamic response values in this period should be chosen as the reference in the subway tunnel design and construction.
4. The pore pressure of saturated soft clay had very distinct response characteristics with the subway traffic load, and closer to the tunnel, the response is more sensitive.
5. The dynamic response of pore pressure in saturated soft clay had hysteresis effect. Besides the distance between measuring point and subway track, it also has some relation to the loading direction.
6. The pore pressure dissipation in saturated soft clay was much slower than the increasing time of pore pressure when subjected to the subway traffic load.

References

Alabi BA (1992) Parametric study on some aspects of ground-borne vibrations due to rail traffic. J Sound Vib 153(1):77–87

Bai B (2003) Pore water pressure of saturated stratum under dynamic impacts. Chin J Rock Mech Eng 22(9):1469–1473 (in Chinese)

Chen S, Xu GB, Gao R (1998) Dynamic analysis of the influence of train railway vibration on building along railways. J North Jiaotong Univ 22(4):57–60 (in Chinese)

Chen MY, Chen RP, Lu S (2002) Some soil mechanics problem in subway construction and operation in soft soil foundation. In: Proceedings of advanced technical forum on urban subway construction and environmental geotechnical. [Editor, Shi P D], Hangzhou, pp 165–177 (in Chinese)

Dassargues A, Biver P, Monjoie A (1991) Geotechnical properties of the quaternary sediments in Shanghai. Eng Geol 31:71–90
Hirokazu T, Shuhei S, Xie WP (2001) Train track-ground dynamics due to high speed moving source and ground vibration transmission. J Struct Mech Earthq Eng 682(7):299–309
Jones CJC, Sheng X, Petyt M (2000) Simulations of ground vibration from a moving harmonic load on a railway track. J Sound Vib 231(3):739–751
Lin YG, Liao SM, Liu GB (2000) A discussion of the factors effecting on longitudinal deformation of subway tunnel. Undergr Space 20(4):264–267 (in Chinese)
Lipen AB, Chigarev AV (1998) The displacements in an elastic half-space when a load moves along a beam lying on its surface. J Appl Maths Mech 62(5):791–796
Okada N, Nemat-Nasser S (1994) Energy dissipation in inelastic flow of saturated cohesionless granular media. Geotechnique 44(1):1–19
Pan CS, Li DW, Xie ZG (1995) Vibration effect of Beijing subway traffic on the environment. J Vib Shock 14(4):29–34 (in Chinese)
Sheng X, Jones CJC, Peryt M (1999) Ground vibration generated by a harmonic load acting on a railway track. J Sound Vib 225(1):3–28
Tang YQ, Huang Y, Ye WM et al (2003a) Critical dynamic stress ratio and dynamic stain analysis of soils around the tunnel under subway train loading [J]. Chin J Rock Mech Eng 22(9):1566–1570 (in Chinese)
Tang YQ, Ye WM, Huang Y (2003b) Marsh gas in shallow soils and safety measures for tunnel construction. Eng Geol 67:373–378
Tang YQ, Zhang X, Zhou NQ (2005) Microscopic study of saturated soft clay's behavior under cyclic loading. J Tongji Univ Nat Sci 33(5):626–630 (in Chinese)
Tang YQ, Yang P, Zhao SK, Zhang X, Wang JX (2008) Characteristics of deformation of saturated soft clay under the load of Shanghai subway line No. 2. Environ Geol 54:1197
Tang YQ, Zhou J, Liu S, Yang P, Wang JX (2010) Test on cyclic creep behavior of mucky clay in Shanghai under step cyclic loading. Environ Earth Sci 63:321–327
Wang CJ, Ji MX, Chen YM (2003) The additional settlement of saturated soft clay foundation under subway loading. In: Proceedings of 9th soil mechanics and geotechnical engineering of Chinese civil engineering. Tsinghua University, Beijing, pp 1118–1122 (in Chinese)
Wang QX, Jiro K, Jiro T (2004) Study on excess pore water pressures of sands mixed with clays under cyclic loading. Chin J Geotech Eng 26(4):541–545 (in Chinese)
Xie N, Sun J (1996) Rheology behavior of Shanghai clays. J Tongji Univ 24(3):233–237
Xie WP, Hu JW, Xu J (2002) Dynamic response of track-ground systems under high speed moving load. Chin J Rock Mech Eng 21(7):1075–1078 (in Chinese)
Xu CJ, Du J, Zhou HB (1997) Establishment of model of pore-water pressure of saturated soft soil under cyclic loading. Shang Geol 3:16–21 (in Chinese)
Xu YS, Shen SL, Du YJ (2009) Geological and hydrogeological environment in Shanghai with geohazards to construction and maintenance of infrastructures. Eng Geol 109:241–254
Yang B, Zhang ZY, Yang NH et al (2002) The analysis of the change of pore-water pressure in soft soil during blasting. Blasting 19(3):8–9 (in Chinese)
Zhang JF, Meng XY (2003) Build-up and dissipation of excess pore water pressure in saturated sand under impact loading. Chin J Rock Mech Eng 22(9):1463–1468 (in Chinese)
Zhang ZY, Lv XL, Chen YQ et al (2003) Experimental study on excess pore water pressure of soils covered by clay layer. Chin J Rock Mech Eng 22(1):131–136 (in Chinese)
Zhou XM, Yuan LY, Cai JQ, Hou XJ (2005) Analysis of soft soil distributed characteristics and deformation examples of Shanghai area. Shanghai Geol 4:6–10 (in Chinese)

http://www.springer.com/978-3-642-41986-7

Dynamic Response and Deformation Characteristic of Saturated Soft Clay under Subway Vehicle Loading
Tang, Y.; Zhou, J.; Ren, X.; Yang, Q.
2014, XXIII, 241 p. 132 illus., 62 illus. in color., Hardcover
ISBN: 978-3-642-41986-7